

Performance Analysis of the HURRAN Tropical Cyclone Forecast System

CHARLES J. NEUMANN¹—Spaceflight Meteorology Group, National Weather Service, NOAA, Miami, Fla.

JOHN R. HOPE—National Hurricane Center, National Weather Service, NOAA, Miami, Fla.

ABSTRACT—The HURRAN (hurricane analog) technique, a fully computerized objective forecast aid making use of past tracks in forecasting hurricane motion, was developed prior to the 1969 hurricane season. Encouraging operational results during the 1969 and 1970 hurricane seasons suggested further evaluation of the technique. To this end, HURRAN computations were made for approximately

1,000 forecast situations. Results are stratified according to initial direction and speed of movement of the sample storms and the number of analogs selected. The utility of the technique is discussed, and the importance of position accuracy at forecast time is demonstrated. Initial indications of the value of the technique are substantiated.

1. INTRODUCTION

The HURRAN (hurricane analog) technique (Hope and Neumann 1970) was used experimentally during the 1969 hurricane season and on an operational basis during the 1970 season. This technique selects analogs from historical tracks and plots their distribution at intervals out to 72 hr. Lines connecting the centroids of these distributions produce the HURRAN forecast track. An example is shown in figure 1. Its demonstrated usefulness has led to this further evaluation and analysis of its performance. Simpson (1971) has asserted that the HURRAN computation is the most conservative predictor of hurricane movement presently available. The National Hurricane Center uses the HURRAN method to objectively identify those areas where a hurricane watch is to be established.

During the 1970 hurricane season, HURRAN computations were made each time an official forecast was issued. The mean 24-hr error for the HURRAN technique was 83 n.mi. and that for the official forecast was 76 n.mi. in 1970, both of which are well below long-term average forecast errors (Tracy 1966, Dunn et al. 1968). For other forecast periods, the HURRAN error was slightly less than the official forecast. It is believed that the HURRAN computations contributed to the below-average errors in the official forecast.

Work is now underway to combine the HURRAN method with the NHC-67 statistical forecasting technique (Miller et al. 1968), the results of which will be reported in a future paper. To initiate this study, HURRAN computations were attempted on approximately 1,000 forecast situations that occurred during tropical storms and hurricanes between 1945 and 1969. The number of

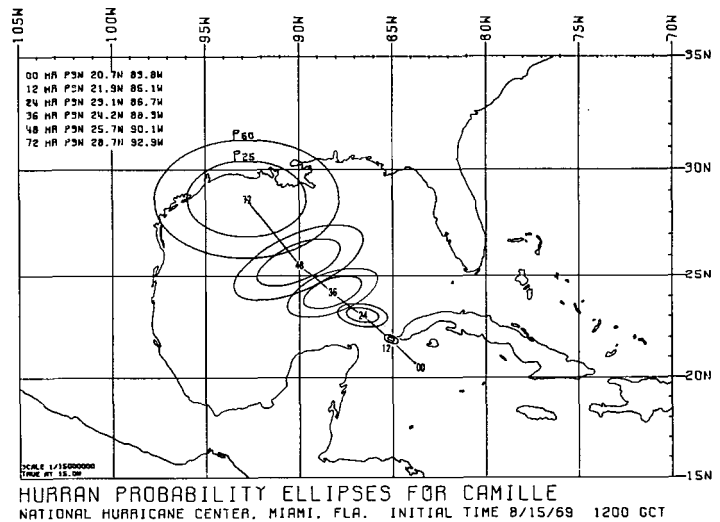


FIGURE 1.—Example of a forecast generated by the HURRAN technique.

times that sufficient analogs were available for HURRAN computations ranged from 628 for 12-hr forecasts to 394 for 72-hr forecasts. The number of cases decreases with time as the storms initially selected move inland, become extratropical, or dissipate. For forecast periods up to 24 hr, it appears that the HURRAN method will yield sufficient analogs for computations approximately two-thirds of the time.

2. PURPOSE

The purpose of this paper is to evaluate the HURRAN results obtained from analysis of this large sample. It will be shown that the goodness of these results is highly dependent upon the initial direction and speed of move-

¹ Present affiliation: National Hurricane Center, National Weather Service, NOAA, Miami, Fla.

TABLE 1.—Summary of HURRAN performance on data for 1945-69

Forecast period (hr)	Type 1 storms (initial W component)					Type 2 storms (initial E component)					Type 3 storms (all cases)				
	12	24	36	48	72	12	24	36	48	72	12	24	36	48	72
Number of cases	403	401	382	367	317	225	220	200	164	77	628	621	582	531	394
Mean error (n.mi.)	24	62	115	180	327	40	125	241	354	556	30	84	158	234	372
Standard deviation of error (n.mi.)	15	37	69	112	226	25	74	132	187	304	21	61	113	161	259
Mean <i>U</i> -component error bias* (n.mi.)	-1	-1	0	-2	9	-1	-4	-25	-25	-46	-1	-2	-9	-9	-2
Mean <i>V</i> -component error bias* (n.mi.)	-2	5	7	8	0	3	0	-5	10	89	2	4	3	9	17
Standard deviation of <i>U</i> -component error (n.mi.)	21	51	95	151	284	34	103	193	282	504	27	74	137	201	338
Standard deviation of <i>V</i> -component error (n.mi.)	19	51	95	149	279	33	103	195	283	376	25	73	138	200	302
Mean absolute value of <i>U</i> -component error (n.mi.)	15	39	73	118	219	26	80	152	225	410	19	54	100	151	256
Mean absolute value of <i>V</i> -component error (n.mi.)	15	41	76	116	210	26	81	155	227	316	19	55	103	150	231

*Forecast minus observed.

ment and dependent to a lesser extent on other factors such as the number of analogs selected and the initial position of the storm. The importance of an accurate estimate of the initial direction and speed of movement and the initial position in using the HURRAN technique will be demonstrated.

A summary of the HURRAN performance on the data sample is shown in table 1. The data have been stratified into three main groups: type 1 storms, those having an initial westerly (W) component of movement and type 2 storms, having an easterly (E) component, while type 3 included both of the other cases. The rationale for this stratification was to separate those storms which had recurved from those which remained in the easterlies. Detailed discussions of the parameters listed in table 1 follow in later sections.

3. DISCUSSION

Figure 2 presents plots of forecast errors versus time for 12, 24, 36, 48, and 72 hr. When the storms were stratified according to initial direction of movement, we found that the HURRAN error for storms initially having an eastward component of movement was nearly twice as great as for those initially having a westward component.

It is very encouraging to discover that the HURRAN method did so well on storms having a westward component of movement because these constituted the bulk of the sample and are the ones most likely to strike populated areas in the United States and adjacent areas. The reasons for the difference in the forecast errors are quite easy to ascertain. Most storms that have a component of movement toward the east have recurved and are beginning to accelerate. At higher forward speed, of course, there is a likelihood of increasing distance error in any forecast system. A detailed analysis of forecast error as related to initial direction and speed of movement is presented later in the paper.

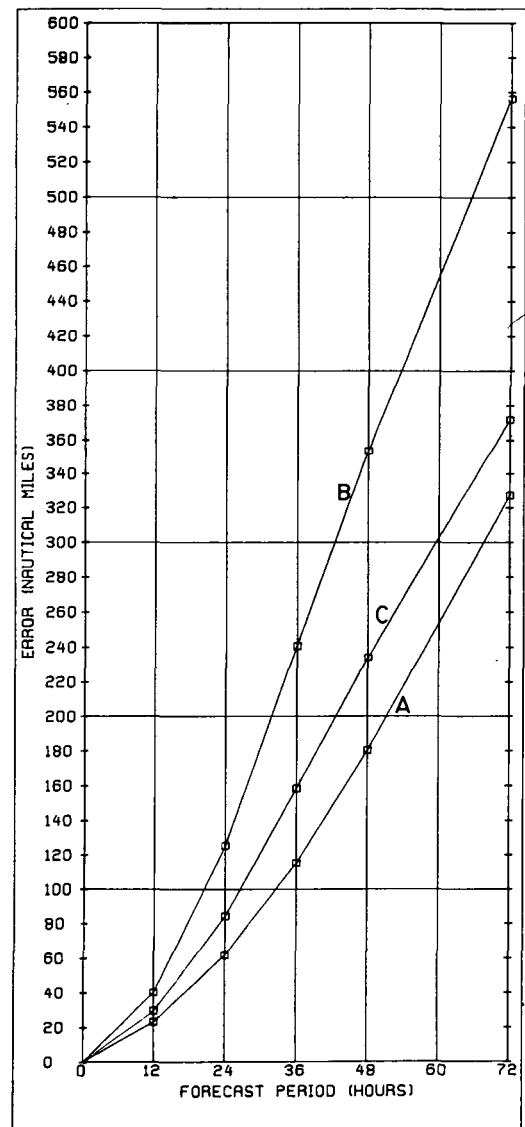


FIGURE 2.—Mean vector error versus time for (A) storms with initial westward movement (type 1), (B) storms with initial eastward movement (type 2), and (C) all storms in the sample (type 3).

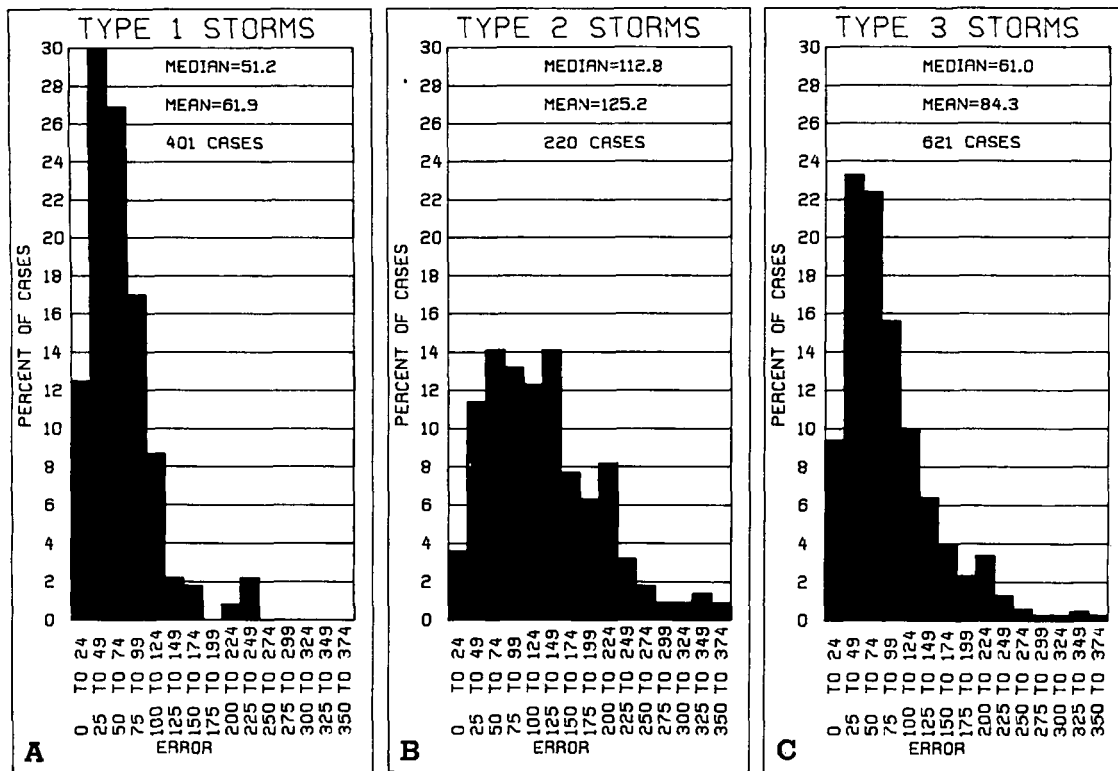


FIGURE 3.—Frequency distribution (percent) of HURRAN 24-hr mean vector errors (n.mi.) for (A) storms with initial westward movement (type 1), (B) storms with initial eastward movement (type 2), and (C) the entire sample (type 3).

We turn now to the 24-hr forecast, a critical one in hurricane forecasting because specific hurricane warnings may be required. The frequency distributions of 24-hr errors for the same three stratifications described above are shown in figure 3. It is apparent from the graphs that the distributions are not univariate normal, and consequently the standard deviation cannot be used to determine, from standard normal tables, the proportion of cases that fall between the mean and various multiples of the standard deviation. The graphs in figure 3 clearly show that the performance of the HURRAN system is considerably better with westward moving storms.

The data shown in figure 4 indicate that the error components (forecast minus observed), or marginal distributions, are normally distributed. Chi-square tests at the 0.05 significance level show that the hypothesis of a normal distribution for the marginals should not be rejected, a necessary condition if a bivariate normal distribution is to be assumed. A discussion of error analysis employing this assumption also follows in a later section.

The mean 24-hr 84-n.mi. error obtained when all 621 cases were considered compares favorably with results generally obtained from the dependent data of other objective forecast techniques (Riehl et al. 1956, Veigas 1959, Miller and Moore 1960, Miller and Chase 1966, Miller et al. 1968). The near 24-hr error of 62 n. mi. from the sample of 401 forecasts of westward moving storms, although very encouraging, cannot be compared directly with other dependent data samples because the stratification is not identical. In the case of storms that were already moving in a direction to the east of due north

(type 2), the 125-n.mi. error for the 24-hr forecast exceeds an acceptable value and certainly can be improved by introducing synoptic parameters.

It should be noted also that in the marginal error distributions (fig. 4) of the HURRAN method there is no significant bias in the 24-hr forecasts; that is, they are distributed about means of near zero. Using the normality assumption, approximately two-thirds (68.26 percent) of the latitude and longitude errors of the HURRAN technique may be expected to be in the ± 50 -n.mi. range in the case of westward moving storms, in the ± 100 -n.mi. range in the case of eastward moving storms, and, considering storms moving in any direction (type 3), about two-thirds of the latitude and longitude errors should fall in the ± 75 -n.mi. range.

Figure 5 shows the error rates for the several forecast periods out to 72 hr. The error rate is defined as the average error over a forecast period divided by the length of the forecast period. Considering the storms initially moving westward (type 1), the error rate increases from 2.6 kt at 24 hr to 4.5 kt at 72 hr, while for eastward moving storms the range is from 5.2 kt at 24 hr to 7.7 kt at 72 hr. The curve consisting of all cases in figure 5 is, of course, the weighted mean of the other two curves. These rates reflect errors in direction as well as in speed.

As was pointed out in Hope and Neumann (1970), the criteria for analog selection can be varied. In operational practice, the National Hurricane Center has selected storms moving in a direction within 22.5° of the track, located within 150 n.mi., and occurring within 15 days of the current storm. If insufficient analogs are obtained, the

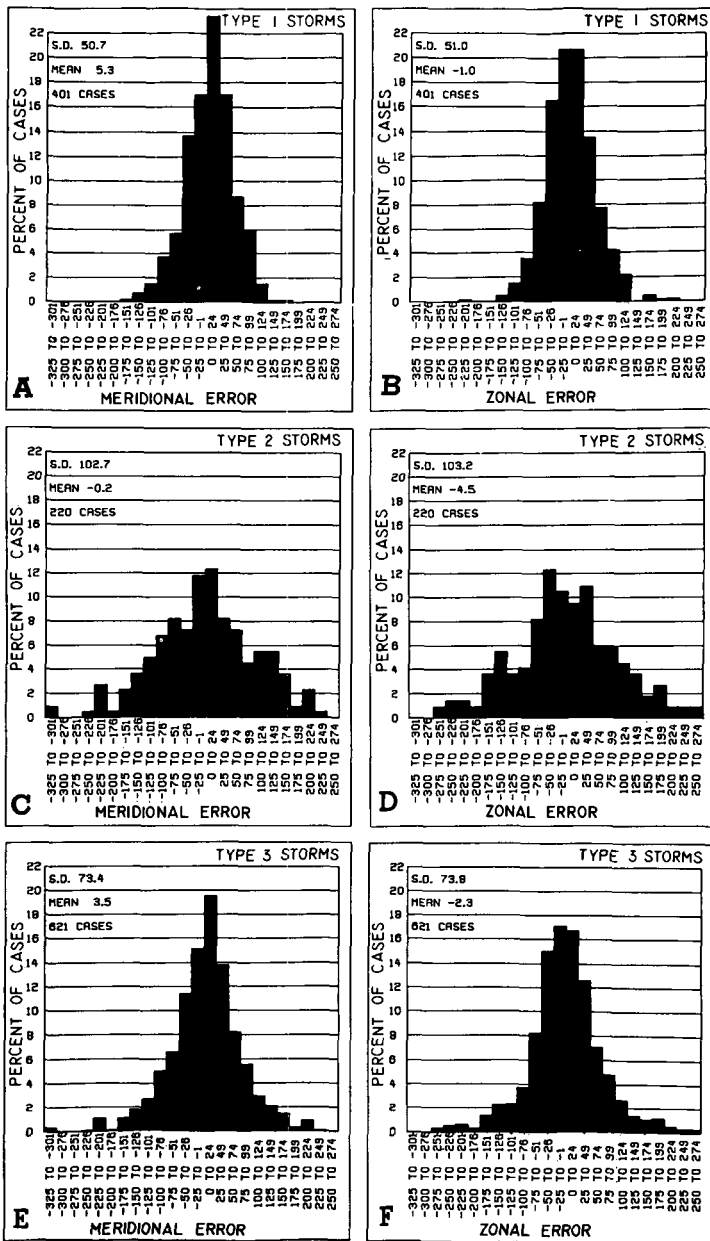


FIGURE 4.—Frequency distribution (percent) of HURRAN 24-hr meridional and zonal component errors (n. mi.) for storms moving initially westward (type 1), (A and B); for storms moving initially eastward (type 2), (C and D); and for all storms in the sample (type 3), (E and F).

criteria can be expanded. The above values employed in operational practice were used initially to obtain the samples in this study, and enough analogs were obtained for 517 24-hr forecasts. The program was then recycled to include storms within 180 n.mi. and within 20 days of the date of the storm for which analogs were sought, resulting in the acquisition of an additional 104 24-hr forecasts. Figure 6 shows that verification results were generally better when smaller selection criteria were employed. However, it is noted that a large portion of the analogs selected under the expanded criteria were storms moving toward the northeast, and the HURRAN errors for that group have been shown to be larger than for storms initially having a westerly component of movement.

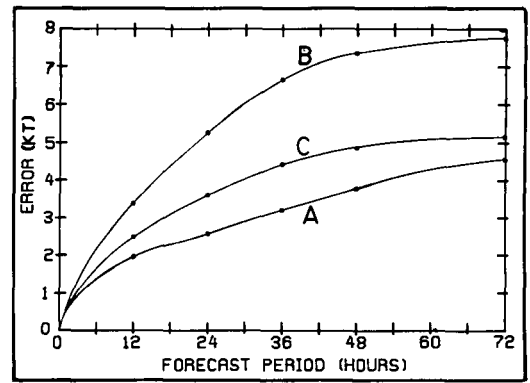


FIGURE 5.—HURRAN vector error rate versus time for (A) storms moving initially westward (type 1), (B) storms moving initially eastward (type 2), and (C) all storms in the sample (type 3).

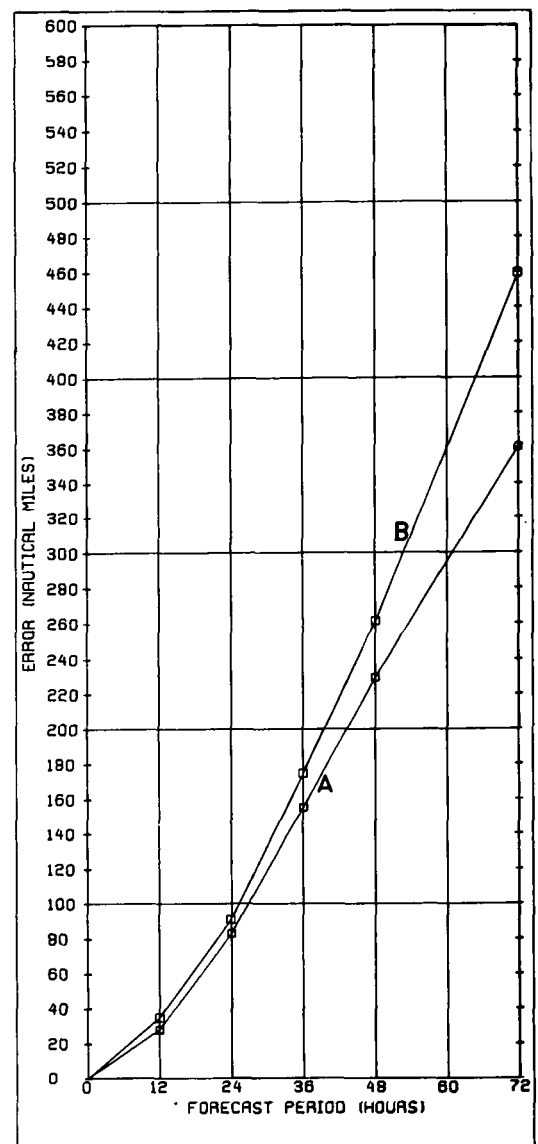


FIGURE 6.—HURRAN vector error versus time for (A) forecasts made from analogs selected within 2.5° of latitude and 15 days either side of date of current storm and (B) forecasts made from analogs selected within 3° of latitude and 20 days either side of date of current storm.

4. FORECAST ERROR VERSUS INITIAL STORM MOVEMENT

In a previous section, it was pointed out that the average absolute forecast error of the HURRAN system was considerably less for storms having an initial westerly component of movement than for those having an initial easterly component. This suggests that the forecast error, E , may be a continuous function of the initial U (longitude) and V (latitude) components of storm motion such that

$$E=f(U,V) \quad (1)$$

where positive U and V refer to eastward and northward motion, respectively. Such a function may be approximated by fitting the N observations of E , U , and V to a third-order polynomial that can be represented as a three-dimensional surface. The general equation of such a surface is given by

$$E=c_1+c_2U+c_3V+c_4UV+c_5U^2+c_6V^2+c_7U^3+c_8U^2V+c_9UV^2+c_{10}V^3. \quad (2)$$

To fit a series of N observations of the dependent variable E and the independent variables U and V to eq (2) by the method of least squares, one must obtain 10 normal equations to solve simultaneously for the most probable values of the 10 unknown constants c_1 through c_{10} . The most probable values of such constants are those which render the square of the residual error a minimum (Mills 1955). The square of the residual error is given by

$$\sum_{i=1}^N [f(U_i V_i) - E_i]^2, \quad (3)$$

where the subscript i refers to individual observations of E , U , and V . Substituting eq (2) into eq (3) gives the expression

$$\sum_{i=1}^N [(c_1+c_2U_i+c_3V_i+c_4U_iV_i+c_5U_i^2+c_6V_i^2+c_7U_i^3+c_8U_i^2V_i+c_9U_iV_i^2+c_{10}V_i^3) - E_i]^2, \quad (4)$$

which must be rendered a minimum.

The 10 normal equations needed to solve for the constants in eq (2) may be obtained by equating to zero the partial derivative of eq (4) with respect to each of the "constants," noting that they are, in fact, really variables until eq (4) is minimized. Following this reasoning, 10 equations are obtained,

$$\Sigma E=c_1N+c_2\Sigma U+c_3\Sigma V+c_4\Sigma UV+c_5\Sigma U^2+c_6\Sigma V^2+c_7\Sigma U^3+c_8\Sigma U^2V+c_9\Sigma UV^2+c_{10}\Sigma V^3, \quad (5)$$

$$\Sigma UE=c_1\Sigma U+c_2\Sigma U^2+c_3\Sigma UV+c_4\Sigma U^2V+c_5\Sigma U^3+c_6\Sigma UV^2+c_7\Sigma U^4+c_8\Sigma U^3V+c_9\Sigma U^2V^2+c_{10}\Sigma UV^3, \quad (6)$$

$$\Sigma VE=c_1\Sigma V+c_2\Sigma UV+c_3\Sigma V^2+c_4\Sigma UV^2+c_5\Sigma U^2V+c_6\Sigma V^3+c_7\Sigma U^3V+c_8\Sigma U^2V^2+c_9\Sigma UV^3+c_{10}\Sigma V^4, \quad (7)$$

$$\Sigma UVE=c_1\Sigma UV+c_2\Sigma U^2V+c_3\Sigma UV^2+c_4\Sigma U^2V^2+c_5\Sigma U^3V+c_6\Sigma UV^3+c_7\Sigma U^4V+c_8\Sigma U^3V^2+c_9\Sigma U^2V^3+c_{10}\Sigma UV^4, \quad (8)$$

$$\Sigma U^2E=c_1\Sigma U^2+c_2\Sigma U^3+c_3\Sigma U^2V+c_4\Sigma U^3V+c_5\Sigma U^4+c_6\Sigma U^2V^2+c_7\Sigma U^5+c_8\Sigma U^4V+c_9\Sigma U^3V^2+c_{10}\Sigma U^2V^3, \quad (9)$$

$$\Sigma V^2E=c_1\Sigma V^2+c_2\Sigma UV^2+c_3\Sigma V^3+c_4\Sigma UV^3+c_5\Sigma U^2V^2+c_6\Sigma V^4+c_7\Sigma U^3V^2+c_8\Sigma U^2V^3+c_9\Sigma UV^4+c_{10}\Sigma V^5, \quad (10)$$

$$\Sigma U^3E=c_1\Sigma U^3+c_2\Sigma U^4+c_3\Sigma U^3V+c_4\Sigma U^4V+c_5\Sigma U^5+c_6\Sigma U^3V^2+c_7\Sigma U^6+c_8\Sigma U^5V+c_9\Sigma U^4V^2+c_{10}\Sigma U^3V^3, \quad (11)$$

$$\Sigma U^2VE=c_1\Sigma U^2V+c_2\Sigma U^3V+c_3\Sigma U^2V^2+c_4\Sigma U^3V^2+c_5\Sigma U^4V+c_6\Sigma U^2V^3+c_7\Sigma U^5V+c_8\Sigma U^4V^2+c_9\Sigma U^3V^3+c_{10}\Sigma U^2V^4, \quad (12)$$

$$\Sigma UV^2E=c_1\Sigma UV^2+c_2\Sigma U^2V^2+c_3\Sigma UV^3+c_4\Sigma U^2V^3+c_5\Sigma U^3V^2+c_6\Sigma UV^4+c_7\Sigma U^4V^2+c_8\Sigma U^3V^3+c_9\Sigma U^2V^4+c_{10}\Sigma UV^5, \quad (13)$$

and

$$\Sigma V^3E=c_1\Sigma V^3+c_2\Sigma UV^3+c_3\Sigma V^4+c_4\Sigma UV^4+c_5\Sigma U^2V^3+c_6\Sigma V^5+c_7\Sigma U^3V^3+c_8\Sigma U^2V^4+c_9\Sigma UV^5+c_{10}\Sigma V^6 \quad (14)$$

where each of the summation signs refers to summation from $i=1$ to N and each of the designates of E , U , and V is subscripted accordingly.

Now designate the 10×10 matrix representing the sums on the right-hand sides of eq (5)–(14) as $A_{j,k}$ where the subscript j refers to the 1–10 rows and k to the 1–10 columns starting in the upper left-hand corner of $A_{j,k}$. Note that element $A_{1,1}$ is given by N , the number of observations. In this case,

$$\sum_{i=1}^N U_i^0 V_i^0 = \sum_{i=1}^N 1 \times 1 = N.$$

Solution of the 10 normal equations by a digital computer is greatly simplified by noting that matrix $A_{j,k}$ is symmetrical about the diagonal element extending from $A_{1,1}$ to $A_{10,10}$ such that

$$A_{j,k}=A_{k,j} \quad k=1, 10; j=k, 10.$$

Therefore, if one of the dimensions of the square matrix is designated by D , the number of terms that need to be evaluated is given by

$$\frac{D(D+1)}{2} = 55$$

rather than 100 if each is evaluated.

A particular solution to eq (2) for the 582 observations of E , U , and V after 36 hr is given by

$$E=126.05+4.81U+2.64V+0.819UV+0.212U^2-0.041V^2-0.0059U^3+0.0051U^2V-0.0616UV^2+0.0189V^3. \quad (15)$$

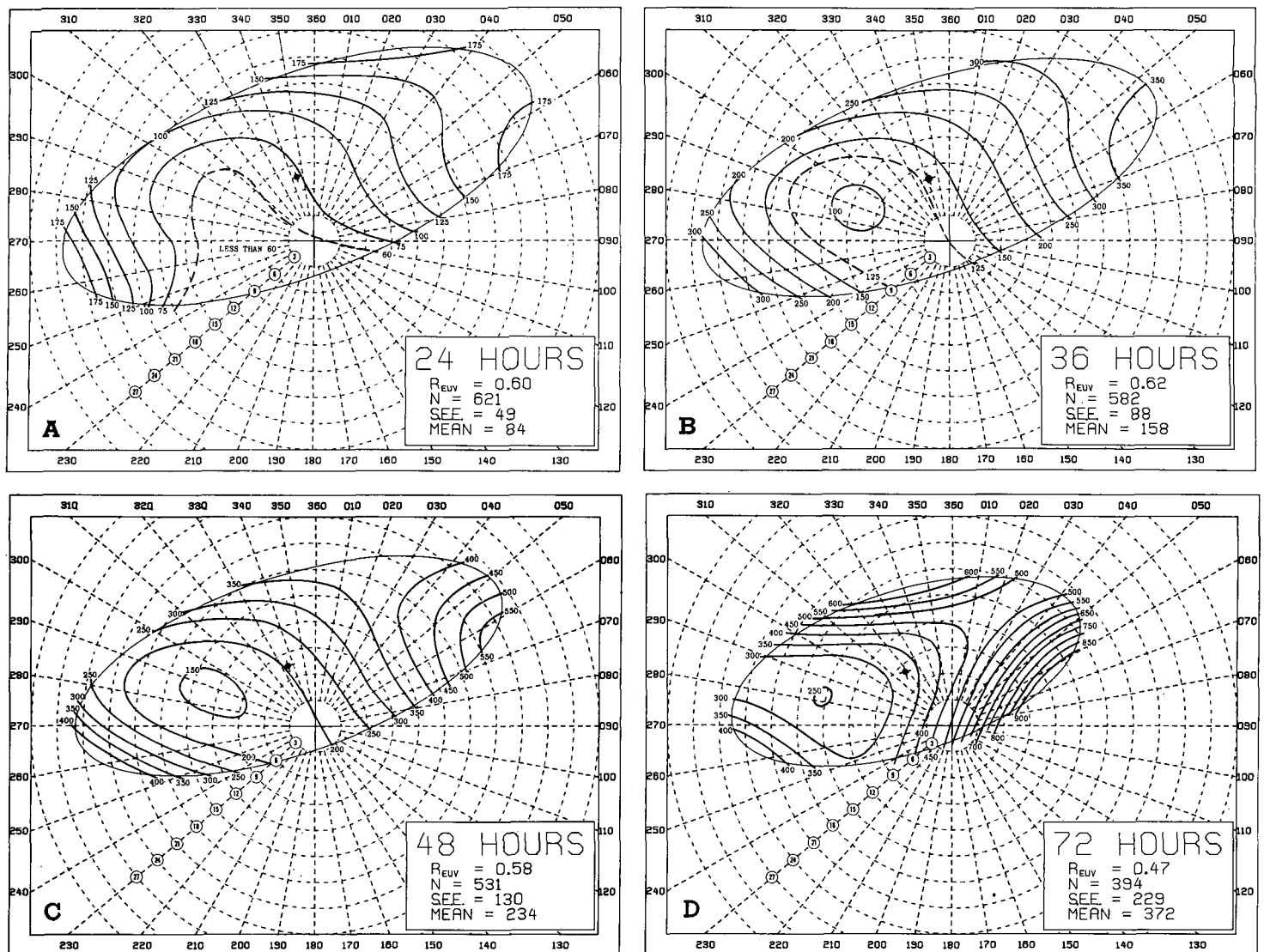


FIGURE 7.—Vector in n.m.i. (solid curves) as a function of initial direction and speed for (A) 24-hr, (B) 36-hr, (C) 48-hr, and (D) 72-hr HURRAN prediction. The radials are storm headings and the concentric circles are spaced at 3-kt intervals. The ellipse is the 99-percent data envelope. Standard errors of estimate and means are in n.m.i.

The multiple correlation coefficient, R_{EUV} , associated with this fit is 0.62. The variance ratio is computed to be 35.5. This latter value is shown to be clearly statistically significant using F -test criteria with the loss of 10 degrees of freedom in fitting eq (2) to the 582 data points (Mills 1955). Bounding of eq (15) is required because, having expressed the error by regression techniques rather than by fitting to a probability distribution, nothing can be inferred outside the range of observations of U and V (Ezekiel 1941). Without bounding, unrealistic values of E might be produced by eq (15), given some unusual observation of U and V . A bounding function is given by the equation of an ellipse in the U, V coordinate system

$$\phi_{99}(U, V) = [(U-h) \cos \theta + (V-k) \sin \theta]^2 / (3.035 SU')^2 + [(V-k) \cos \theta - (U-h) \sin \theta]^2 / (3.035 SV')^2 \quad (16)$$

where θ is the angle of rotation of the major axis of the ellipse from the positive U -axis, h and k are the centroids (mean U and mean V) of the ellipse, and SU' and SV' are

the standard deviations of the U and the V components along the major and minor axes, respectively. Values of SU' , SV' , and θ are obtained by fitting the array of all U and V components to a bivariate normal distribution. Details of this fitting process are given in Hope and Neumann (1970). The constant 3.035 is chosen such that 99 percent of the observations should be included in the resultant ellipse.

For the 36-hr ellipse, the value of θ is computed to be 19.1° ; the standard deviation of the U components along the major axis, SU' , is 9.1 kt and the standard deviation of the V components along the minor axis, SV' , is 3.6 kt. The centroid (mean U and V) is given by $(-2.4, 7.2)$. Substituting these values in eq (16), one gets for the bounding function

$$\phi_{99}(U, V) = 0.00208U^2 + 0.00778V^2 - 0.00448UV + 0.0420U - 0.1222V + 0.487 \quad (17)$$

The ellipse on figure 7B represents the locus of all U and V

TABLE 2.—Expected 36-hr HURRAN forecast error (n.mi.) as a function of initial storm movement and position. The last column shows the HURRAN error as a function of initial direction and speed only.

Storm movement (deg./kt)	Initial position							
	15.0°N 70.0°W	18.0°N 82.5°W	25.0°N 90.0°W	25.0°N 85.0°W	15.0°N 55.0°W	20.0°N 65.0°W	22.5°N 75.0°W	
270/12	96	117	70	102	83	130	137	111
280/12	79	97	82	104	81	103	115	97
290/12	79	89	96	107	96	88	101	96
300/12	95	94	110	113	129	85	94	100
310/12	126	109	126	122	179	95	96	111
320/12	167	132	142	132	241	117	106	124

values obtained by setting eq (17) to unity. The analysis of the error within the elliptical bounds is given by the solution of eq (15) over the range of the observed U and V components. No smoothing was accomplished; the analysis is precisely as given by eq (15).

The analyses on figures 7A–7D confirm the earlier finding that the error in the HURRAN process is closely related to the initial direction of movement, and show also that the error is related to the initial speed. The solid lines in these figures are isolines of error, the dashed concentric circles are speeds in increments of 3 kt, and the dashed radials are directions toward which the storms are moving. For example, after 24 hr, storms moving initially in a general westerly or northwesterly direction can be expected to have an error less than 75 n.mi. Consider specifically an initial movement of 310 degrees at 18 kt; figure 7A then shows an error of about 80 n.mi. Because the standard error of estimate (S.E.E.) for 24 hr is 49 n.mi., the 24-hr error for storms moving with that direction and speed may be expected to be in the range 80 ± 49 n.mi. approximately two-thirds of the time. Similar interpretations can be made for any initial direction and speed falling within the various ellipses. The bold-dotted cross mark located at the center of the ellipse on each chart represents the resultant direction and speed vector of all storms making up the sample. Note that the ellipse shifts progressively southwestward with time. This occurs because the number of cases also decreases with time and the ones that are lost are most frequently those that were initially moving northeastward.

The analysis on figures 7A–7D showed the forecast error as a joint function of the orthogonal components of initial storm motion as indicated by eq (1). It should be expected that the error, E , might also be a function of other parameters such as time, t , as given by day number, and the initial latitude, L_a , and initial longitude, L_o , such that,

$$E=f(U,V,t,L_a,L_o) \quad (18)$$

where U and V have the same meaning as in eq (1). It was determined by regression analysis that the inclusion of t in eq (18) did not significantly reduce the error variance, but that an additional 6 percent reduction in

variance was realized by the inclusion of L_a and L_o . Therefore,

$$E=f(U,V,L_a,L_o) \quad (19)$$

was expanded in polynomial form using the same rationale used in expanding eq (1) into eq (2) except that 35 normal equations must be formulated rather than the 10 given by eq (5)–(14).

The first 7 columns of table 2 give particular solutions to the polynomial expansion of eq (19). The last column gives the error as a function of U and V alone as shown in figure 7B. The table shows, for example, that a storm located in the Caribbean Sea at 15°N, 70°W and moving toward 280° at 12 kt would be better forecast by the HURRAN system than a storm located just north of Hispaniola at 22.5°N and 75.0°W. The data in table 2 suggest that forecasts made on storms that depart from normal storm tracks for a given area result in larger forecast errors using the HURRAN system.

This analysis shows at once the strength and weakness of the HURRAN method. For storms moving westward and northwestward at forecast time, which has been shown to be most often the case, the accuracy of the method is clearly demonstrated. For those moving toward the northeast, it is evident that other information has to be considered to reduce the error to an acceptable value.

5. DISTRIBUTION OF ERRORS

Figures 8–10 are plots of the HURRAN errors for the categories discussed previously; initial westward component (type 1), initial eastward component (type 2), and the combination including all the storms of the sample (type 3). Each plotted point represents the end point of an individual vector error. Probability ellipses 0.10 through 0.90, which assume a bivariate normal distribution similar to those presented by Tracy (1966), have been fitted to these data. In these figures, the concentric circles (dashed) specifying distance are centered at the origin, which has been placed at the mean of the observed positions for each forecast period. The large cross mark is located at the computed mean of the forecast positions. The difference between the means of the observed and forecast positions is a measure of the bias of the system. This value (in n.mi.) is printed out at the lower right of

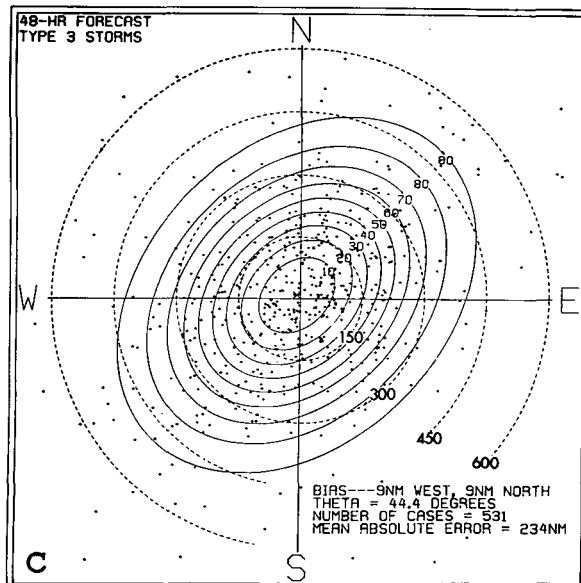
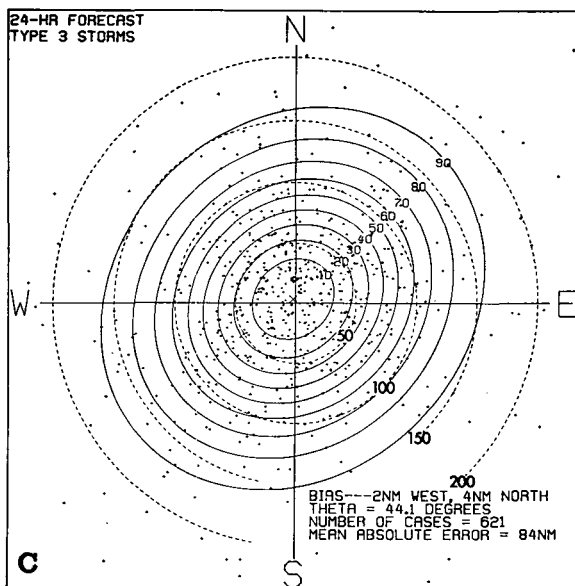
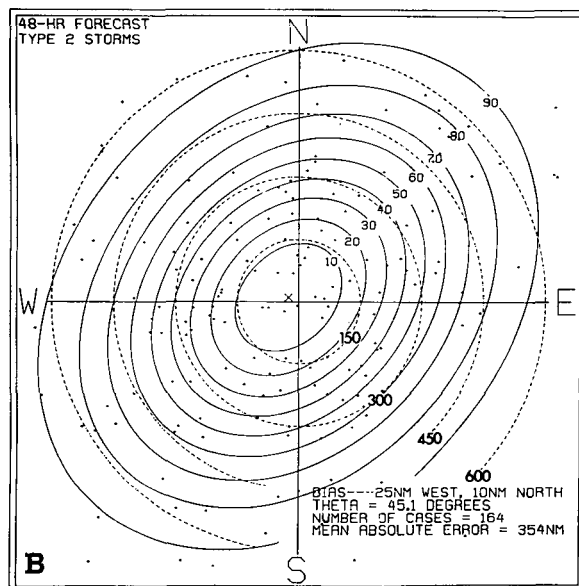
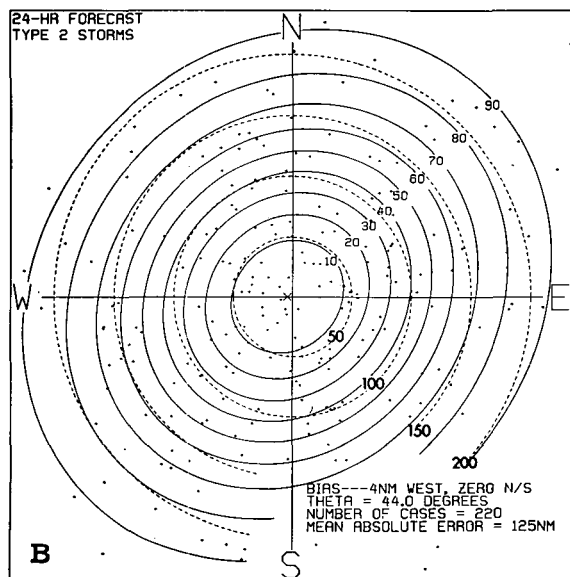
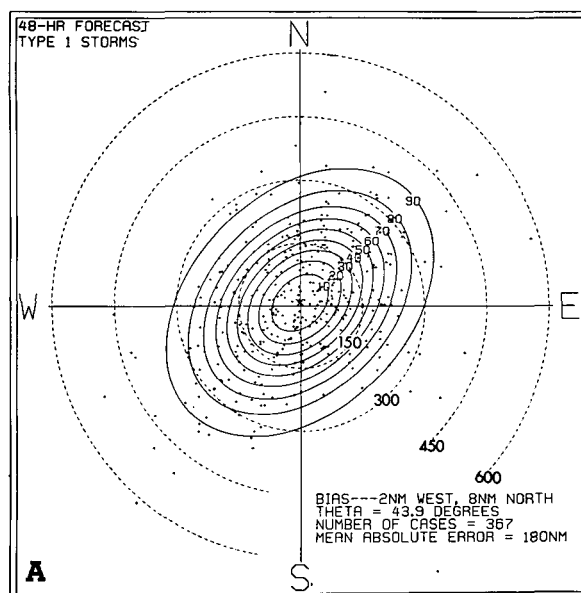
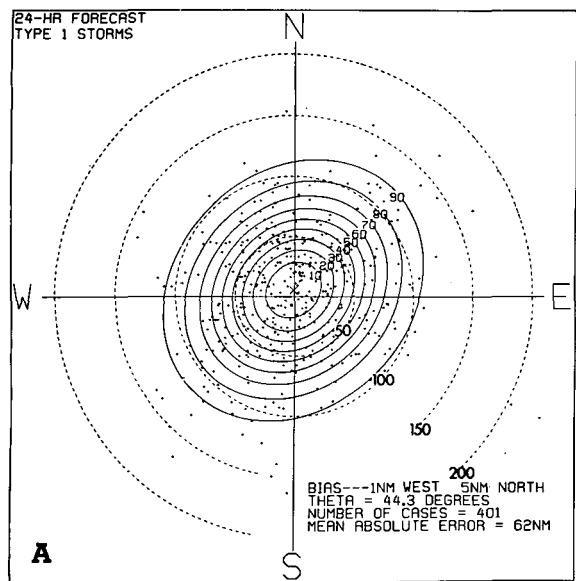


FIGURE 8.—Plot of 24-hr forecast errors (n.mi.) and fitted probability ellipses for (A) storms with initial westward movement (type 1) (B) storms with initial eastward movement (type 2), and (C) all storms in the sample. Scale (given by dashed concentric circles), biases, and mean absolute errors are in n.mi.

FIGURE 9.—Same as figure 8 except 48 hr.

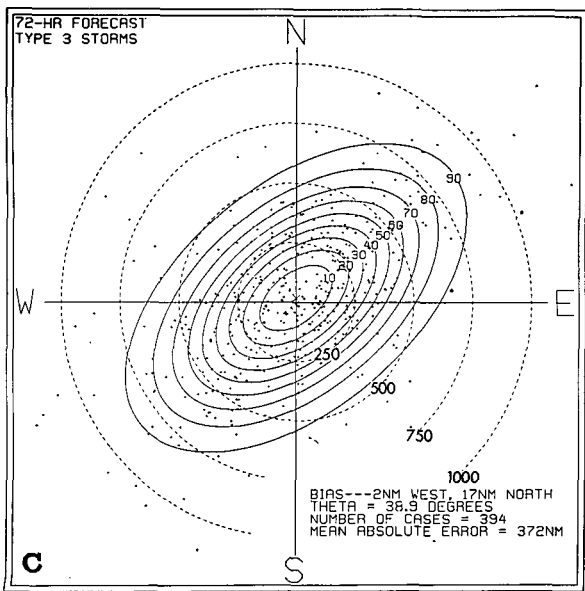
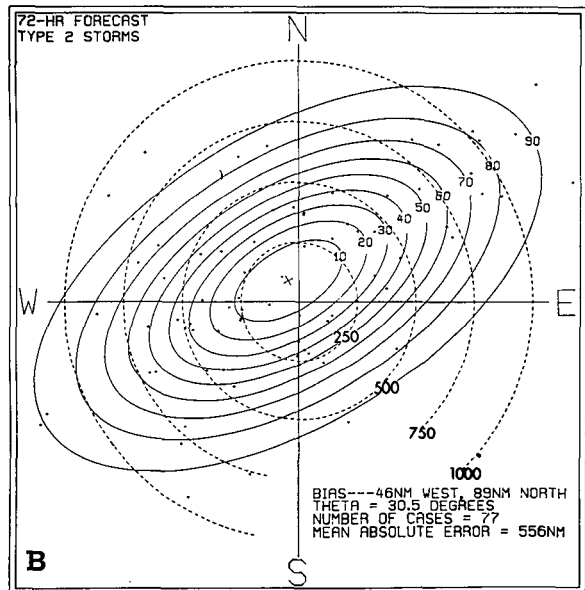
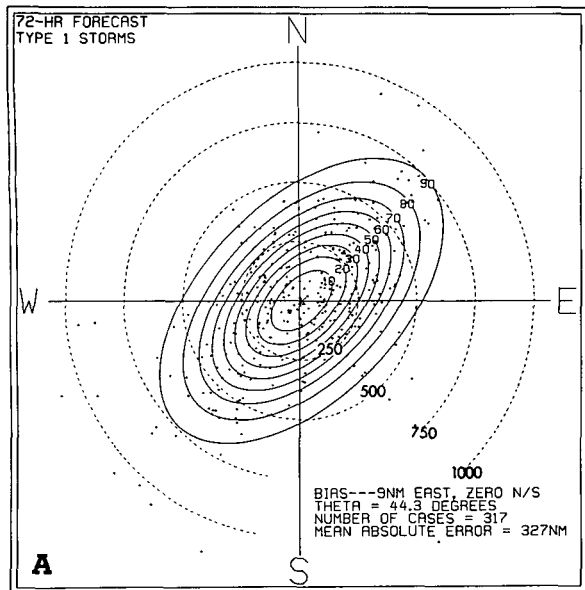


FIGURE 10.—Same as figure 8 except 72 hr.

each figure. As can be seen from examination of the figures, the bias is very small compared to the magnitude of the errors. The only significant bias to appear was at 72 hr with storms moving with an initial component toward the east (fig. 10B). Here, the east-west bias was about 46 n.mi. and the north-south bias was about 89 n.mi. That is, the HURRAN method in this circumstance forecast, in the mean, storms to be located about 46 n.mi. too far west and 89 n.mi. too far north in 72 hr. Examination of individual cases of the storms that made up this sample leads one to the conclusion that of the 87 storms in this category that were lost between 48 and 72 hr, a large percentage continued to accelerate northeastward and were no longer classified as tropical storms or hurricanes as they acquired extratropical characteristics over the cold waters of the north Atlantic, or else moved beyond the area of consideration.

For any given forecast period, the ellipses in figures 8-10 are drawn to the same scale. Note that the type 1 ellipses are approximately one-fourth the area of the type 2 ellipses. This again demonstrates clearly that the HURRAN system produces more reliable results when storms are initially moving in a direction with a westerly component.

In certain instances, it may be desirable to determine the probability contained in some portion of these ellipses. Precise methods of integrating the bivariate normal probability density function to obtain this probability have been outlined by several authors (e.g., Groenewoud et al. 1967). Graphical methods of approximating this value have been described by Neumann (1969) and Chase (1969).

6. TOTAL FORECAST ERROR AS A FUNCTION OF DIRECTION AND SPEED ERROR

One of the stated purposes of this paper is to demonstrate the need for accuracy in estimating the position, direction, and speed of movement of tropical storms and hurricanes at forecast time. As is well known, only slight errors in forecast direction and speed when accumulated over a period of time can result in rather substantial misses at the end of a forecast period. This is illustrated in figure 11, the curves of which were computed from the law of cosines, showing the total error in a forecast as a function of direction error, speed error, actual storm speed, and time. For example, figure 11A shows that for storms actually moving at 10 kt, a direction error of 10° and a forecast speed 4 kt too slow will result in a 24-hr error of just over 100 n.mi., while an error of 10° and 4 kt too fast will result in a slightly larger error. This difference is accentuated by larger direction and speed misses; an error of 25° and 8 kt too slow will yield a 24-hr miss of just under 200 n.mi., while an error of 25° and 8 kt too fast will produce an error of nearly 250 n.mi. In general, then, forecasts that are too fast yield larger errors than those that are too slow, given the same direction error. At 72 hr, figure 11F shows that an error of only 10° and 5 kt too fast produces a 450-n.mi. error when a storm actually moves at 20 kt for the period.

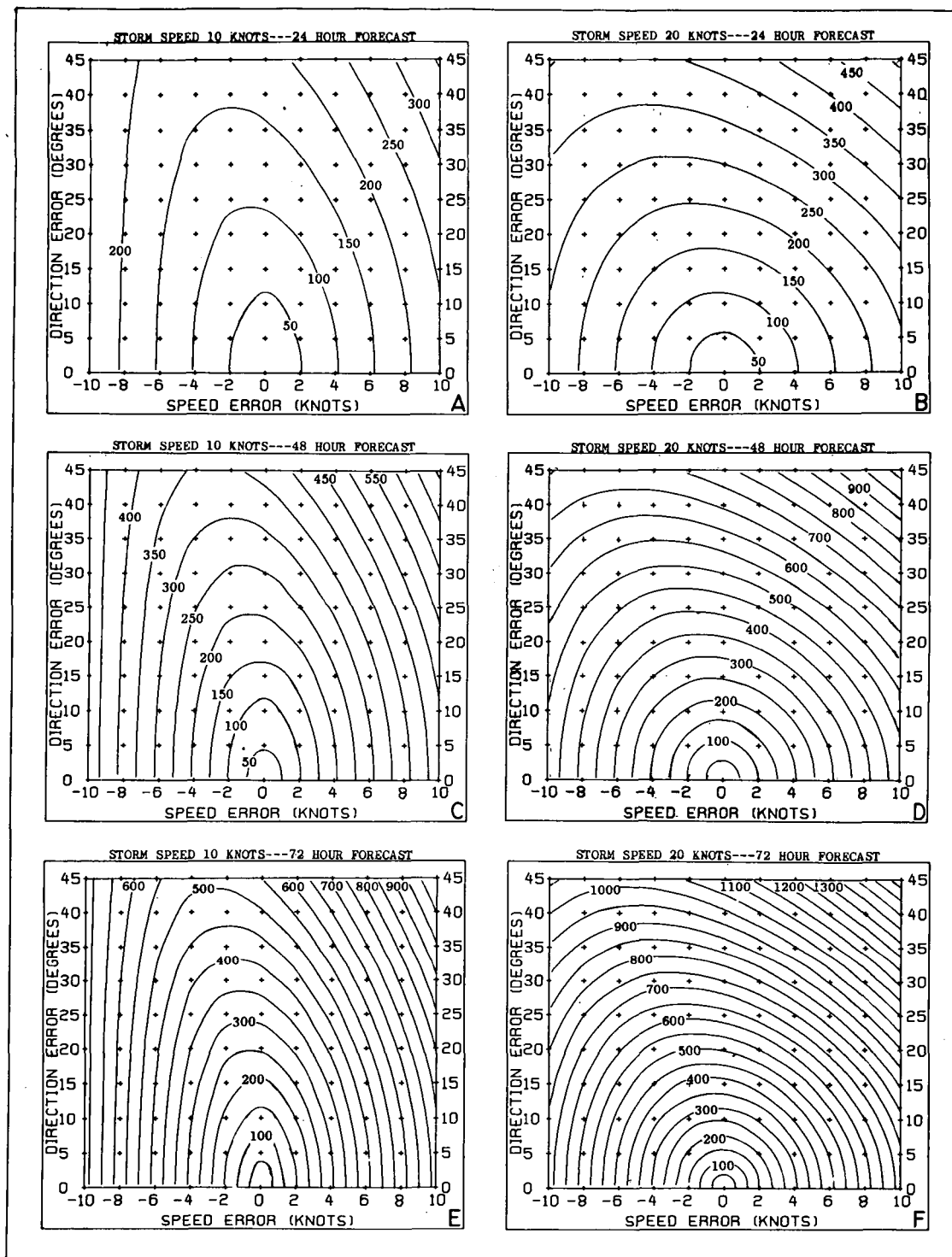


FIGURE 11.—Total forecast error as a function of direction and speed error for specified periods and actual storm speeds.

7. IMPORTANCE OF INITIAL POSITION ACCURACY

A further illustration demonstrates the sensitivity of the HURRAN computations to the initial input. Slight deviations from the best track of hurricane Carla of 1961 in the Gulf of Mexico were inserted into the HURRAN program and the resulting tracks were plotted (fig. 12). The "bogus" directions and speeds were obtained by systematically shifting the current position and the one 6 hr earlier to the left and right, respectively, of the best-track

positions in increments of 5, 10, 20, and 30 n.mi., then reversing the directions of displacement to the right at the current time and to the left 6 hr earlier. Finally, the current and 6 hr earlier positions were displaced along the track in opposite directions by these same increments. For each pair of displacements, the heading and speed were computed and fed into the program as initial conditions. The resulting spread of the tracks shown in figure 12 clearly illustrates the necessity of accuracy of the input into the HURRAN program.

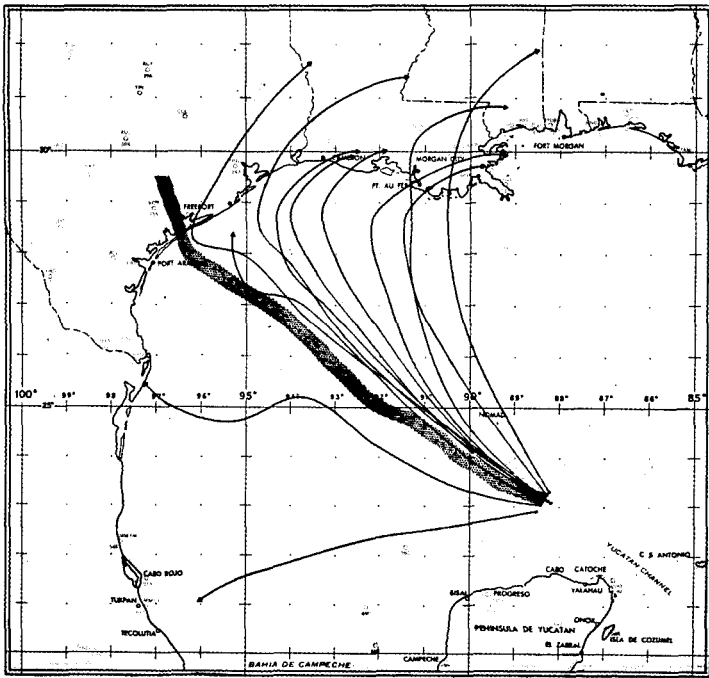


FIGURE 12.—Spread of HURRAN tracks resulting from shifting of position at forecast time and position 6 hr earlier related to hurricane Carla of 1961. Shaded track is actual path of Carla.

8. SUMMARY

The foregoing analysis demonstrates that the HURRAN method produces forecasts that compare favorably with any objective system and with official forecasts themselves, especially when the forecasts are made prior to recurvature of the storms. The increased dispersion of accelerating storms after recurvature results in larger errors in the system by about a factor of two. It is known that other forecast systems encountered this same difficulty.

The performance of the HURRAN technique in a particular case can be estimated in advance as it has been shown to be correlated with the initial direction and speed of movement and with the location of the storm.

Although the accuracy of the HURRAN computations increases when the number of analogs selected increases, it does so only by a small amount.

On the average, sufficient analogs will be selected for the HURRAN computations about two-thirds of the time for forecast periods up to 24 hr. This proportion may be expected to increase over the years as additional storms are added to the historical records.

The sensitivity of the HURRAN technique to accuracy of initial conditions demands that the input parameters be determined with great care.

9. CONCLUSION

The analysis of a large sample of HURRAN forecasts confirmed earlier indications that the technique is a

valuable tool for the hurricane forecaster. Its success suggests that the environmental flow patterns associated with tropical storms or hurricanes moving within a small range of direction, speed, and location, and occurring within limited portions of the hurricane season, usually have much in common, initially, and their evolution frequently proceeds in an analogous manner.

ACKNOWLEDGMENTS

The authors express their appreciation to the National Hurricane Research Laboratory for the computer time and facilities required to obtain the HURRAN forecasts used in the study. We are grateful to Elbert Hill of the National Hurricane Center for providing the contour program to analyze the error fields in figure 11.

REFERENCES

- Chase, Peter P., "A Note on Drawing Probability Sectors," *Monthly Weather Review*, Vol. 97, No. 8, Aug. 1969, pp. 602-603.
- Dunn, Gordon E., Gentry, R. Cecil, and Lewis, Billy M., "An Eight-Year Experiment in Improving Forecasts of Hurricane Motion," *Monthly Weather Review*, Vol. 96, No. 10, Oct. 1968, pp. 708-713.
- Ezekiel, Morderai, *Methods of Correlation Analysis*, John Wiley & Sons, Inc., New York, N.Y., 1941, 531 pp. (see pp. 347-349).
- Groenewoud, C., Hoaglin, D. C., Vitalis, John A., and Crutcher, Harold L., "Bivariate Normal Offset Circle Probability Tables With Offset Ellipse Transformations," *CAL Report XM-2464-G-1*, 3 vols., Cornell Aeronautical Laboratory, Inc., Buffalo, N.Y., Dec. 15, 1967, 1364 pp.
- Hope, John R., and Neumann, Charles J., "An Operational Technique for Relating the Movement of Existing Tropical Cyclones to Past Tracks," *Monthly Weather Review*, Vol. 98, No. 12, Dec. 1970, pp. 925-933.
- Miller, Banner I., and Chase, Peter P., "Prediction of Hurricane Motion by Statistical Methods," *Monthly Weather Review*, Vol. 94, No. 6, June 1966, pp. 399-406.
- Miller, Banner I., Hill, Elbert C., and Chase, Peter P., "A Revised Technique for Forecasting Hurricane Movement by Statistical Methods," *Monthly Weather Review*, Vol. 96, No. 8, Aug. 1968, pp. 540-548.
- Miller, Banner I., and Moore, P.L., "A Comparison of Hurricane Steering Levels," *Bulletin of the American Meteorological Society*, Vol. 41, No. 2, Feb. 1960, pp. 59-63.
- Mills, Frederick C., *Statistical Methods*, Holt, Rinehart, and Winston, Inc., New York, N.Y., 1955, 842 pp. (see pp. 727-731).
- Neumann, Charles J., "Probability of Tropical Cyclone Induced Winds at the NASA Manned Spacecraft Center," *ESSA Technical Memorandum WBTM SOS-4*, Weather Bureau, U.S. Department of Commerce, Washington, D.C., May 1969, 46 pp.
- Riehl, Herbert, Haggard, William H., and Sanborn, Richard W., "On the Prediction of 24-Hour Hurricane Motion," *Journal of Meteorology*, Vol. 13, No. 5, Oct. 1956, pp. 415-420.
- Simpson, Robert H., "The Decision Process in Hurricane Forecasting," *Technical Memorandum NWS SR 53*, National Weather Service, Southern Region, U.S. Department of Commerce, Miami, Fla., Jan. 1971, 35 pp.
- Tracy, Jack D., "Accuracy of Atlantic Tropical Cyclone Forecasts," *Monthly Weather Review*, Vol. 94, No. 6, June 1966, pp. 407-418.
- Veigas, Keith W., Miller, Robert G., and Howe, George M., "Probabilistic Prediction of Hurricane Movement by Synoptic Climatology," *Occasional Papers in Meteorology* No. 2, The Travelers Insurance Co., Hartford, Conn., June 1959, 54 pp.

[Received May 27, 1971; revised December 21, 1971]